

Stranski-Krastanov Mode in Iron Electrodeposition

M. Saitou

Department of Mechanical Systems Engineering, University of the Ryukyus, 1 Senbaru Nishihara-cho Okinawa, 903-0213, Japan

E-mail: saitou@tec.u-ryukyu.ac.jp

Received: 9 Decemebr 2016 / Accepted: 6 January 2017 / Published: 12 February 2017

The morphological transition of iron thin films generated by a rectangular pulse current technique having a frequency ranging from 0.1 to 1 MHz was investigated using scanning electron microscope (SEM) and X-ray diffraction (XRD). An increase in the film thickness of the iron thin film grown on an ITO glass was found to cause two types of the Stranski-Krastanov (S-K) mode: the forward S-K mode that the two-dimensional growth changes into the three dimensional growth first appeared, and the reverse S-K mode that the three dimensional growth changes into the two-dimensional growth secondly appeared. A critical film thickness at which the S-K mode transition occurs was several orders of magnitude larger than that reported in vapor phase epitaxy. In addition, an increase in the deposition temperature also caused the reverse S-K mode. XRD analysis revealed that the S-K mode took place owing to the competition between the dominant (211) plane and the (110) plane. The iron thin film composed of only the (211) plane parallel to the ITO glass was generated.

Keywords: forward Stranski-Krastanov, reverse Stranski-Krastanov, iron thin film, critical film thickness

1. INTRODUCTION

Iron thin films have recently attracted researchers owing to a new potential application of the surface magnetism such as an interplay between an ultra-thin iron film and substrate, surface anisotropy, and transition to a spin glass state [1-7]. For example, a correlation between the magnetic behavior and the morphology of nanostructured iron materials is investigated to understand the origin of the attractive magnetic property.

To prepare the iron thin film, an electrodeposition technique is a simple and low cost method. Many kinds of solutions in iron electrodeposition [8-9] have been proposed to generate the iron deposits. Electrochemical parameters that affect the morphology of the iron thin film [10-14] were

reported. The initial growth in electrodeposition follows the Volmer-Weber mode [8], i.e., isolated iron nuclei generated on a substrate coalesce together to form a thin film as crystallization proceeds. The iron thin film comprises columnar grains and pores [13-15], which indicates that the surface morphology is far from the smooth surface. The (100), (110), and (211) crystallographic planes grown parallel to the substrate were also reported to exist in the iron thin film. However, in electrodeposition, there have been very few studies on the Stranski-Krastanov mode [16-20] that indicates a transition from the two-dimensional growth to the three-dimensional growth. This is because the three-dimensional growth already governs at an initial stage in the thin film growth reported in the previous studies. The Stranski-Krastanov mode is known to be very useful for the fabrication of quantum dots [18-20].

In body centered cubic (BCC) metals such as iron electrodeposits, the surface energy becomes smaller in order of the (100), (211), and (110) plane [21]. However, the (110) plane is not always observed as a dominant crystallographic plane grown parallel to the substrate. In electrodeposition, the exchange current density dependent on the crystallographic plane is shown to play an important role in the appearance of the crystallographic plane other than the (110) plane [17-18]. In general, a high index plane that has the large exchange current density enables the deposited film to grow at a high growth rate. Hence, the high index plane parallel to the substrate tends to appear at a high current density in electrodeposition [15, 23]. However, at present, we have no phenomenological theory to describe the surface morphology far from equilibrium.

As reported in the reference [24], a pulse electrodeposition technique has several advantages in comparison with a direct current electrodeposition technique. The low frequency below 1 kHz has been applied in electrodeposition. However, recently, in nickel electrodeposition at a rate of megahertz [25], an energy level transition between an electron at the Fermi energy level in an electrode and a nickel ion characterized by a quantized rotational energy level was found. Electrodeposition at a rate of megahertz was employed to generate the iron thin film in this study.

In the present study, we demonstrate that the iron thin film indicates the forward and reverse S-K mode and the transitions are related to the instability of the (211) and (110) crystallographic planes.

2. EXPERIMENTAL SET UP

An ITO glass of 15x10 mm² and carbon plate of 35x40 mm² were prepared for a cathode and anode electrode. A solution including 1.25 mol/L ferrous sulfate heptahydrate (Fe₂SO₄ · 7H₂O) and 0.86 mol/L potassium sodium tartrate tetrahydrate (C₄H₄KNaO₆ · 4H₂O) was employed. The solution was strained using a membrane with a pore size of 0.1 μm and maintained in electrodeposition at a temperature ranging from 287 to 323 K.

The rectangular pulse voltage at a frequency ranging from 0.1 to 1 MHz and an amplitude ranging from 12.5 to 35.8 mA/cm² was supplied with a function generator. A metal film resistor of 22 Ω was connected in series with an electrochemical cell comprising the two electrodes and solution. To calculate the rectangular pulse current carried between the two electrodes, a voltage drop at the metal film resistor was measured with a digital oscilloscope. Figure 1 shows a plot of a typical rectangular

pulse current at a frequency of 1 MHz, which was carried in the solution at a temperature of 302 K to generate the iron thin film. The current on-time was chosen to be equal to the current off-time.

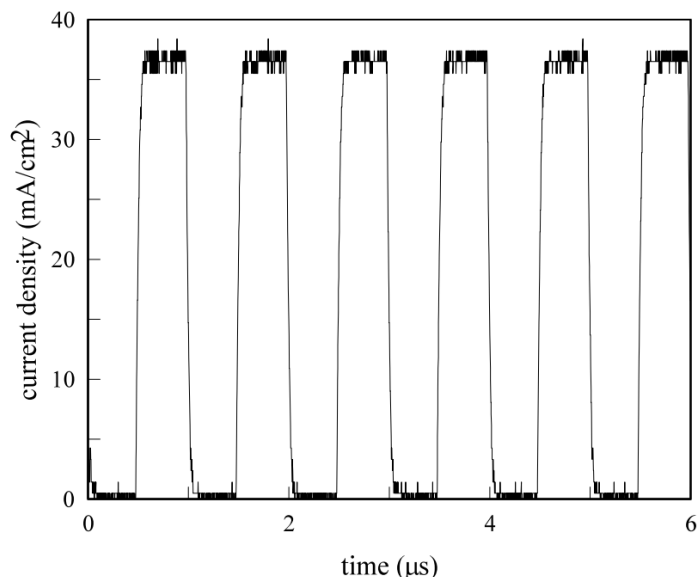


Figure 1. A plot of the rectangular pulse current having an amplitude of 35.8 mA/cm^2 and a frequency of 1 MHz.

After electrodeposition, the iron thin film generated on the ITO glass was rinsed with distilled water and put into a vacuum chamber to avoid oxidization. The iron thin film was observed with SEM (Hitachi TM3030). The conventional XRD (Rigaku Ultima) with $\text{CuK}\alpha$ radiation and a standard θ - 2θ diffractometer with a monochromator of carbon was used to identify the crystallographic structure of the iron thin film on the ITO glass.

3. RESULTS AND DISCUSSION

3.1 Forward and reverse S-K mode transition

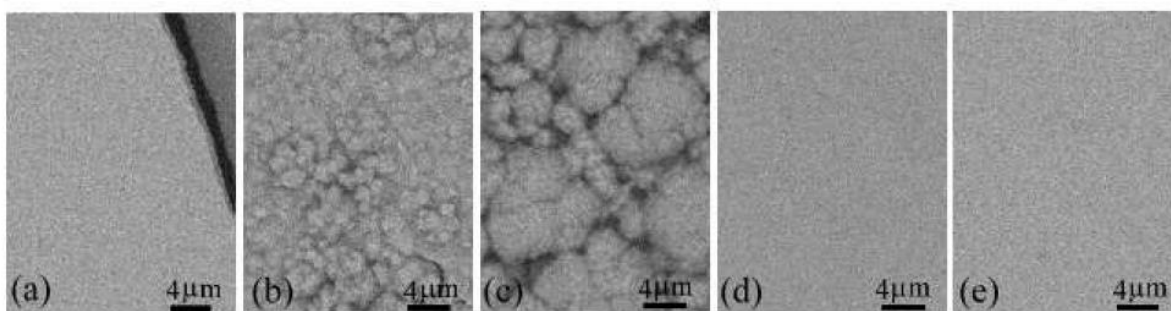


Figure 2. SEM images of the iron thin films generated at an amplitude of 22.3 mA/cm^2 , a frequency of 1 MHz, and a temperature of 302 K. The iron thin film had a film thickness of (a) $3 \mu\text{m}$, (b) $6 \mu\text{m}$, (c) $10 \mu\text{m}$, (d) $14 \mu\text{m}$, and (e) $19 \mu\text{m}$.

Figure 2 shows typical SEM images of the iron thin film generated at an amplitude of 22.3 mA/cm², a frequency of 1 MHz, and a temperature of 302 K. The film thickness of the iron thin film increases in order of alphabet in Fig. 2. Figure 2 (a) shows the smooth surface and the fracture edge to prove that the image is in focus. It is noted that the SEM images in Figs. 2 (d) and (e) are also in focus. Figure 2 (b) shows the rough surface comprising grains in contrast with the smooth surface in Fig. 2 (a). The transition named as the forward S-K mode that means a transition from the two-dimensional growth (layer by layer growth) to the three-dimensional growth [16] occurs.

The surface in Fig. 2 (c) comprises grains as well as that in Fig. 2 (b). The surface in Fig. 2 (d) again becomes the smooth surface. The transition named as the reverse S-K mode that means a transition from the three-dimensional growth to the two-dimensional growth occurs. There have been no studies on the S-K transition in electrodeposition as far as we know.

According to the theoretical treatment of the forward S-K mode in vapor phase epitaxy [16, 26], the forward S-K mode transition is caused by the competition between the free energy composed of the binding energy (related to an interaction between an adatom and the nearest neighbor atoms) and the strain energy, and the entropy. At a critical film thickness, the forward S-K transition takes place to lessen the free energy that increases with the film thickness. The value of the critical film thickness is in general about several nanometers or several monolayers [18-19].

On the other hand, in iron electrodeposition, as shown in Figs. 2 (a) and (b), the critical thickness is several orders of magnitude larger than that in vapor phase epitaxy. The strain energy due to a lattice mismatch between the grown layer and the substrate caused the cracks in Fig. 2 (a). The binding energy can be approximately replaced with the surface energy and the edge energy of steps in the surface [19]. The crystallographic plane in the iron thin film, which is related to the surface energy, was investigated with XRD.

The reverse S-K mode has not been found in vapor phase epitaxy and electrodeposition as far as we know. However, as shown in Figs. 2 (c) and (d), the three-dimensional growth was found to change into the two-dimensional growth. The iron thin film in Fig. 2 (d) had a thickness of 16 μm. In the framework of the forward S-K mode in vapor phase epitaxy, the free energy minimum requires the transition from the three-dimensional growth to the two-dimensional growth to decrease the free energy. In this study, two kinds of the critical film thickness for the forward and reverse S-K transition are found to describe the S-K mode transition.

Figure 3 shows a typical XRD chart of the iron thin film. The three diffraction peaks are consistent with those by the crystallographic planes of polycrystalline α-iron. No other peak diffracted by materials other than iron is observed. So as to investigate a change in the crystallographic plane with the film thickness, the texture coefficient $T(hkl)$ defined by the following equation is used,

$$T(hkl) = \frac{I(hkl)_i / I_o(hkl)_i}{\sum_N I(hkl)_i / I_o(hkl)_i}, \quad (1)$$

where $I(hkl)_i$ is the measured intensity of the (hkl) diffraction, $I_o(hkl)_i$ is the standard intensity of polycrystalline α-iron [27] and N is the total number of a diffraction peak. The texture coefficient indicates the ratio of the crystallographic planes in the iron thin film parallel to the substrate.

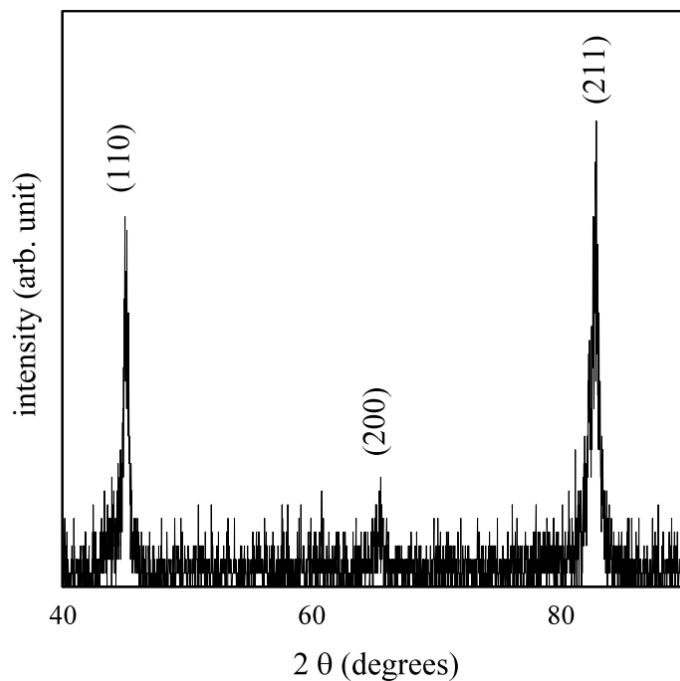


Figure 3. XRD chart of the iron thin film generated at an amplitude of 22.3 mA/cm², a frequency of 1 MHz, and a temperature of 302 K.

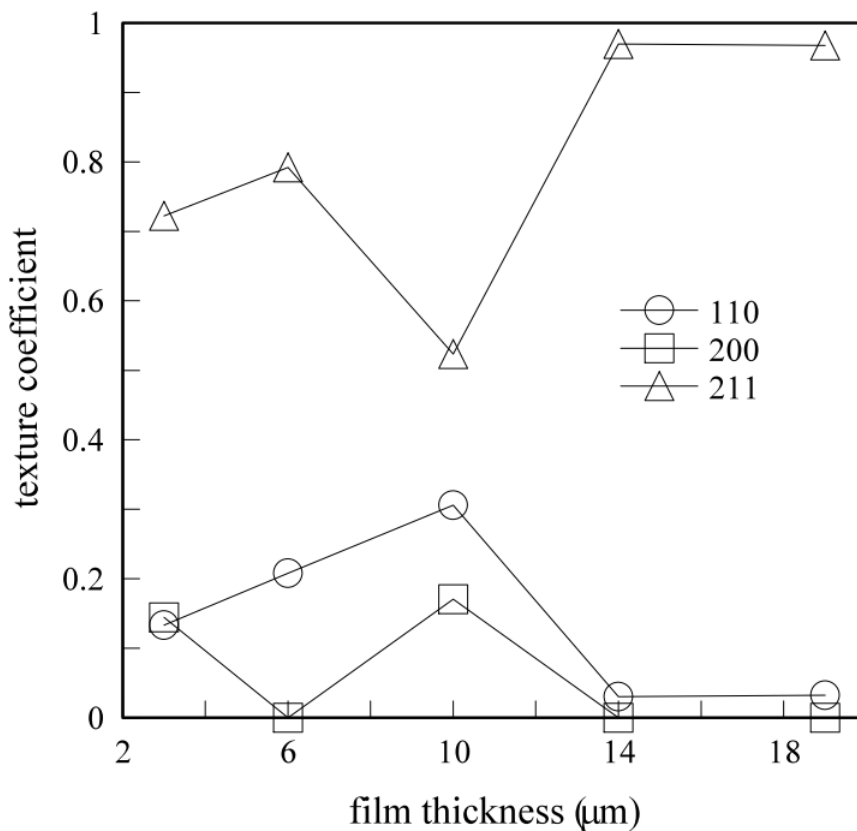


Figure 4. A plot of the texture coefficient vs. the film thickness of the iron thin film generated at an amplitude of 22.3 mA/cm², a frequency of 1 MHz, and a temperature of 302 K.

Figure 4 shows a plot of the texture coefficient vs. the film thickness. A large change in the texture coefficients of the (211) and (110) plane occurs at a film thickness between 6 and 14 μm . The S-K modes observed with SEM takes place in the same region ranging from 6 to 14 μm .

According to calculations based on the density functional theory [21], the surface energy of the (211) plane with a packing fraction of 0.481 is larger than that of the (110) plane. The appearance of the crystallographic plane parallel to the substrate does not obey the surface energy minimum. In electrodeposition, the exchange current density involved with the growth rate plays an important role in the surface morphology. In general, a high index plane has the large exchange current density in comparison with a low index plane. Hence, the high index plane parallel to the substrate often emerges at the high current density [22]. This is different from the crystallographic plane observed in the vapor phase epitaxy.

In the iron thin film, the presence of the (211) increases the surface energy. On the other hand, the entropy that increases owing to the low packing decreases the free energy. The competition between the binding energy and entropy determines the critical film thickness according to the model of the forward S-K mode. In iron electrodeposition, the large critical film thickness might indicate a small difference between the two energies.

Figure 5 shows a plot of the grain size vs. the film thickness. The grain size was determined from the (110) diffraction peak using the Scherrer equation [22]. The grain size does not increase with the film thickness within a variance. This indicates that the grain growth saturates or extremely slows. In a field of thin films [28-29], this phenomenon is called the stagnant columnar structure. All the grain boundaries in the film intersect the surface and the interface between the film and substrate. Owing to the low spatial resolution of the SEM used in this study, the presence of the columnar structure could not be ascertained. No increase in the grain size in Fig. 5 allows the surface roughness that keeps constant even at a large film thickness. In fact, in Fig. 2 (e) the surface of the iron thin film having a film thickness of 19 μm shows smooth and appears mirror-like.

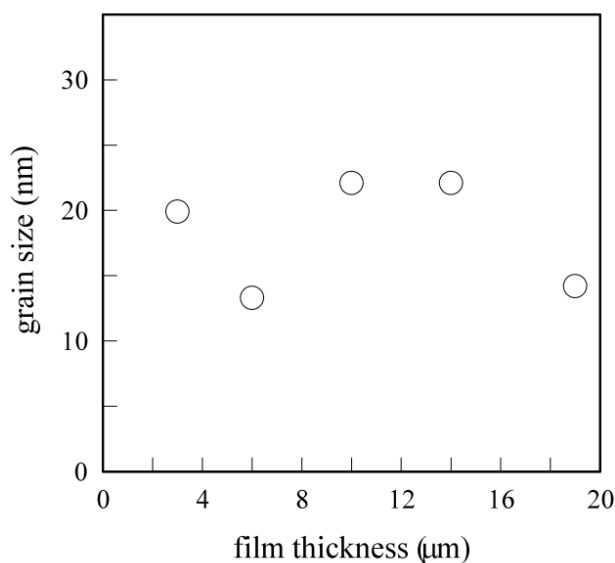


Figure 5. A plot of the grain size vs. the film thickness of the iron thin film generated at an amplitude of 22.3 mA/cm^2 , a frequency of 1 MHz, and a temperature of 302 K.

3.2 Reverse S-K mode transition dependent on the deposition temperature

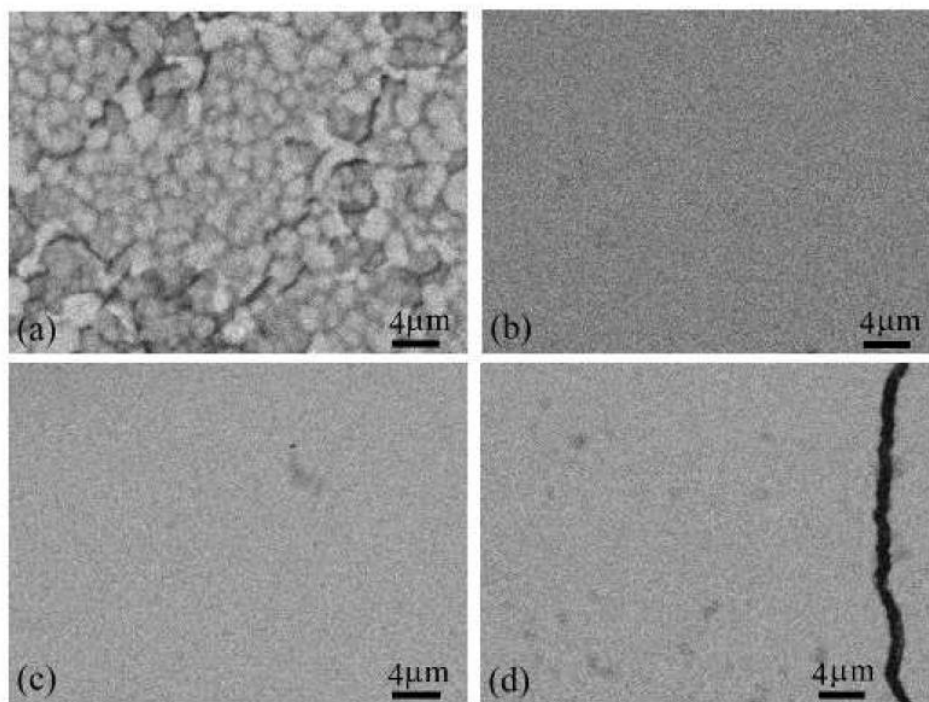


Figure 6. SEM images of the iron thin films generated at an amplitude of 22.3 mA/cm^2 , a frequency of 1 MHz, and a temperature of (a) 288 K, (b) 296 K, (c) 312 K, and 323 K. The iron thin film had a film thickness of $3 \text{ }\mu\text{m}$.

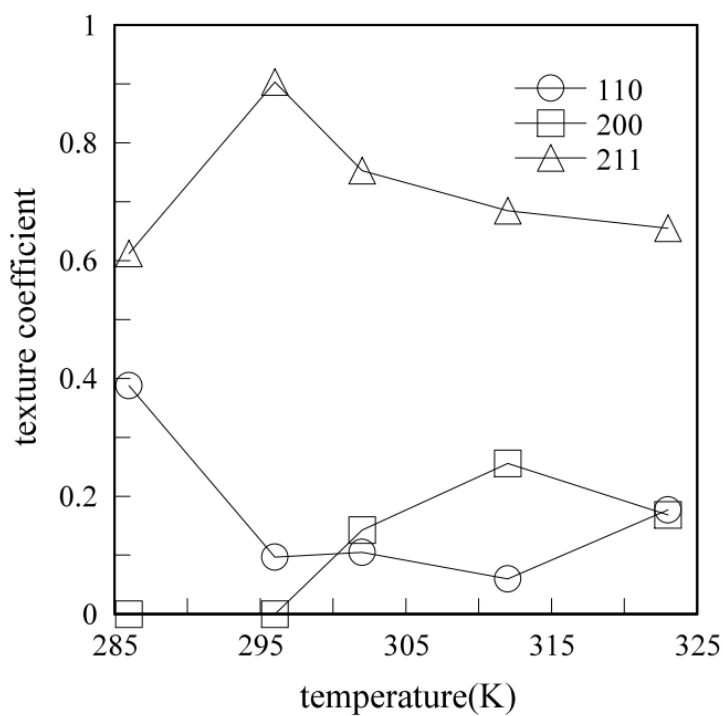


Figure 7. A plot of the texture coefficient vs. the temperature. The iron thin film was generated at an amplitude of 22.3 mA/cm^2 and a frequency of 1 MHz.

Figure 6 shows SEM images of the iron thin films generated at a temperature of (a) 288 K, (b) 296 K, (c) 312 K, and (d) 323 K. The fracture cross-section of the film in Fig. 6 (d) is shown to be the SEM image in focus. At a deposition temperature of 288 K, the SEM image of the iron film shows an aggregation of grains. The smooth surface in Fig. 6 (b) indicates that the reverse S-K mode takes place with an increase in the deposition temperature. The critical film thickness in the forward S-K transition in vapor phase epitaxy is dependent on the deposition temperature [30] owing to the entropy related to the surface configuration.

Figure 7 shows a plot of the texture coefficient vs. the deposition temperature. A large change in the texture coefficients of the (211) and (110) planes occurs at a temperature ranging from 288 to 296 K. As shown in Fig. 6, in the same temperature range from 288 to 296 K, the reverse S-K mode transition takes place.

3.3 Smooth surface morphology independent of the frequency

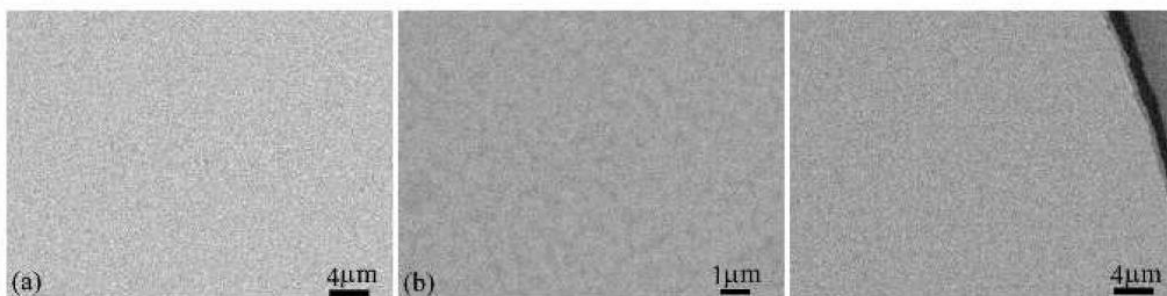


Figure 8. SEM images of the iron thin films generated at an amplitude of 22.3 mA/cm² and a temperature of 312 K, and a frequency of (a) 0.1 MHz, (b) 0.6 MHz, and (c) 1 MHz.

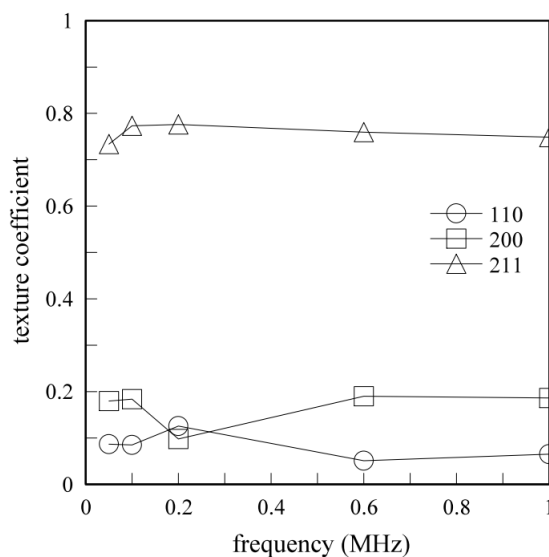


Figure 9. A plot of the texture coefficient vs. the frequency. The iron thin film was generated at an amplitude of 22.3 mA/cm² and a temperature of 312 K.

Figure 8 shows SEM images of the iron thin films generated at a frequency ranging from 0.1 to 1 MHz. The fracture cross-section of the film in Fig. 8 (c) is shown to be the SEM image in focus. Irrespective of the frequency, the iron film shows the smooth surface that appears mirror-like. The megahertz frequency is expected to affect the deposition mass in electrodeposition. If the resonant frequency at which the deposition mass rapidly increases exists at a frequency ranging from 0.1 to 1MHz as well as that in nickel electrodeposition [25], the forward S-K mode may be suppressed by an increase in the growth rate. As shown in Fig. 8, the surface appears smooth and stable.

Figure 9 shows a plot of the texture coefficient vs. the frequency. A texture change between the (200) and the (110) plane takes place at 0.2 MHz, however, the value of the texture coefficient of the (211) plane almost keeps constant.

3.4 Smooth surface morphology independent of the current density

Figure 10 shows SEM images of the iron thin films generated at a current density ranging from 12.5 to 35.8 mA/cm². The fracture cross-section of the iron thin film in Fig. 10 (c) is shown to be the SEM images in focus. Irrespective of the current density, the iron film shows the smooth surface that appears mirror-like.

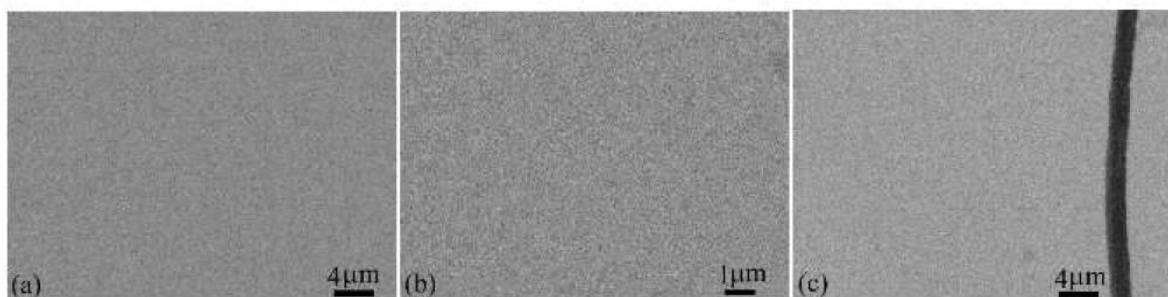


Figure 10. SEM images of the iron thin films generated at a frequency of 1 MHz and a temperature of 302 K, an amplitude of (a) 12.5 mA/cm², (b) 22.3 mA/cm², and (c) 35.8 mA/cm².

Figure 11 shows a plot of the texture coefficient vs. the current density. The (211) plane is a stable and dominant crystallographic plane at a current density ranging from 12.5 to 35.8 mA/cm². The texture coefficient of the (211) plane above 0.92 indicates that the (211) plane parallel to the ITO glass is almost occupied in the iron thin film. The (110) plane that has the smallest surface energy [21] is formed in the vicinity of the ITO glass surface at the initial stage. The value of the (211) texture coefficient above 0.92 indicates that the iron thin film comprising only the (211) plane is generated at a site distant from the surface of the ITO glass. At a far lower current density, the low index plane will be dominant. In electrodeposition, not only the surface energy, but also the exchange current density is involved with the dominant crystallographic plane in growth [22].

Thus, when the competition between the (211) plane and (110) plane occurs in iron electrodeposition, it is concluded that the S-K mode transition takes place.

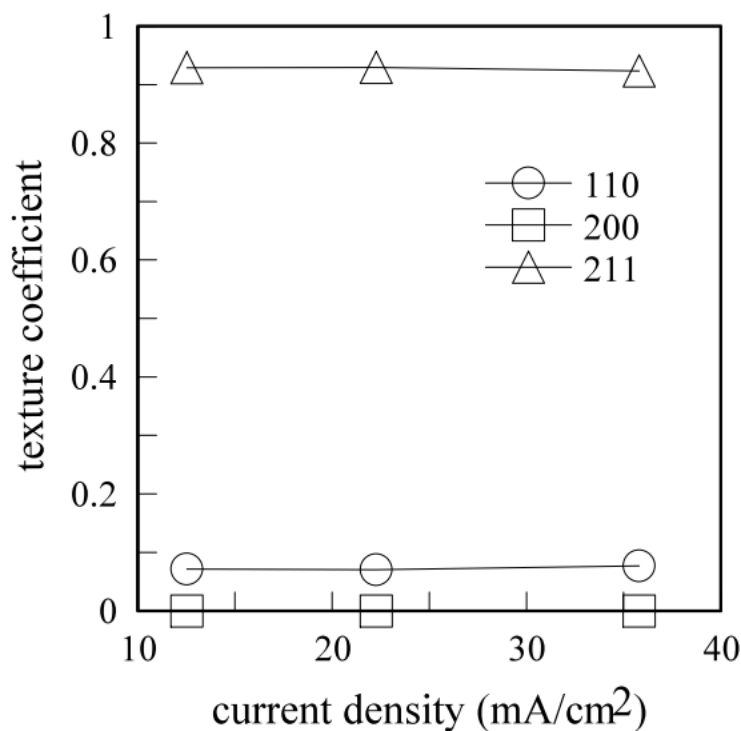


Figure 11. A plot of the texture coefficient vs. the current density. The iron thin film was generated at a frequency of 1 MHz and a temperature of 302 K.

4. CONCLUSIONS

The S-K mode transition of the iron thin film generated by the rectangular pulse current technique was investigated using scanning electron microscope (SEM) and X-ray diffraction (XRD). The S-K mode transition was found to be composed of the forward S-K mode and the reverse S-K mode. With an increase in the film thickness of the iron thin film, the forward S-K and the reverse S-K mode appeared in order. With the increase in the deposition temperature, only the reverse S-K mode transition appeared. The XRD analysis revealed that the S-K mode took place when the dominance of the (211) plane was disturbed by the (110) plane. The iron thin film composed of only the (211) plane parallel to the ITO glass was generated at a frequency of 1 MHz, a temperature of 302 K, and a current density above 12.5 mA/cm².

References

1. M. Mebarki, A. Layadi, M. R. Khelladi, A. Azizi, N. Tiercelin, V. Preobrazhensky, and P. Pernod, *Metall. Mater. Trans. A*, 47A (2016) 3677.
2. R. Brajpurriya, *J. Appl. Phys.*, 107 (2010) 083914.
3. B. Ghebouli, S.-M. Chérif, A. Layadi, B. Helifa, M. Boudissa, *J. Magn. Magn. Mater.*, 312 (2007) 194.

4. A. Gündel, T. Devolder, C. Chappert, J. E. Schmidt, R. Cortes, and P. Allongue, *Physica B* 54 (2004) 282.
5. G. Herzer, *J. Magn. Magn. Mater.*, 294 (2005) 99.
6. E. Jartych, D. Chocyk, M. Budzyński, M. Jałchowski, *Appl. Surf. Sci.*, 180 (2001) 246.
7. M. Mebarki, A. Layadi, A. Guittoum, A. Benabbas, B. Ghebouli, M. Saad, and N. Menni, *Appl. Surf. Sci.*, 257 (2011) 7025.
8. D. Grujicic and B. Pesic, *Electrochim. Acta* 50 (2005) 4405.
9. E. A. Abd El Meguid, S. S. Abd El Rehim, and E. M. Moustafa, *Thin Solid Films*, 443 (2003) 53.
10. M.W. -Żołopa, E. Grądzka, K. Szymański, and K. Winkler, *Thin Solid Films*, 548 (2013) 44.
11. Yu. A. Ivanova, J. F. Monteiro, A. L. Horovistiz, D. K. Ivanou, D. Mata, R. F. Silva, and J. R. Frade, *J. Appl. Electrochem.*, 45 (2015) 515.
12. K. V. Gow and G. J. Hutton, *Electrochim. Acta*, 17 (1972) 1797.
13. K. H. Kim, J. D. Lee, J. J. Lee, B. Y. Ahn, H. S. Kim, and Y.W. Shin, *Thin Solid Films*, 483 (2005) 74,
14. K. Inoue, T. Nakata, and T. Watanabe, *Mater. Trans.*, 43 (2002) 1318.
15. F. A. Harraz, T. Sakka, and Y. H. Ogata, *Electrochim. Acta*, 50 (2005) 5340.
16. A. Baskaran and P. Smerek, *J. Appl. Phys.*, 111 (2012) 044321.
17. Yu. N. Drozdov, D. N. Lobanov, A. I. Nikiforov, A. V. Novikov, V. V. Ul'yanov, and D. V. Yurasov, *J. Surf. Invest.: X-Ray, Synchrotron Neutron Tech.*, 3 (2009) 548.
18. T. Walther, D. J. Norris, Y. Qiu, A. Dobbie, M. Myronov, and D. R. Leadley, *Phys. Status Solidi A*, 210 (2013) 187.
19. G. Chen, B. Sanduijav, D. Matei, G. Springholz, D. Scopece, M. J. Beck, F. Montalenti, and L. Miglio, *PRL*, 108 (2012) 055503.
20. O. T. Ogurtani, A. Celik, and E. E. Oren, *J. Appl. Phys.*, 115 (2014) 224307.
21. J. -M. Zhang, F. Ma, and K. -W. Xu, *Surf. Interface Anal.*, 35 (2003) 662.
22. M. Saitou, *Int. J. Electrochem. Sci.*, 11 (2016) 6491.
23. T. Hurlen, *Acta Chem. Scand.*, 14 (1960) 1533.
24. C. Larson and J. P. G. Farr, *Trans. Inst. Met. Finish.*, 90 (2012) 20.
25. M. Saitou, *Int. J. Electrochem. Sci.*, 11 (2016) 5535.
26. R. J. Asaro and W. A. Tiller, *Metall. Trans.*, 3 (1972) 1789.
27. JCPDS-ICDD Card No. 06-0696.
28. C. V. Thompson, *Annu. Rev. Mater. Sci.*, 20 (1990) 245.
29. I. Petrov, P. B. Barna, L. Hultman, and J. E. Greene, *J. Vac. Sci. Technol. A*, 21 (2003) 117.
30. L. Sfaxi, L. Bouzaiene, H. Sghaier, and H. Maaref, *J. Cryst. Growth*, 293 (2006) 330.